The oncogenic potential of Kaposi's sarcoma-associated herpesvirus cyclin is exposed by p53 loss in vitro and in vivo

Emmy W. Verschuren,[1] Juha Klefstrom,[1] Gerard I. Evan,[1,3] and Nic Jones[2]

[1]Cancer Research Institute, University of California, San Francisco, San Francisco, California 94115
[2]Paterson Institute for Cancer Research, Christie Hospital NHS Trust, Manchester M20 4BX, United Kingdom
[3]Correspondence: gevan@cc.ucsf.edu

Summary

Expression of the Kaposi's sarcoma-associated herpesvirus (KSHV) cyclin D homolog, K cyclin, is thought to contribute to viral oncogenesis. We show that K cyclin expression in primary cells sensitizes to apoptosis and induces growth arrest, both of which are dependent on p53 but independent of E2F1 or p19^{ARF}. DNA synthesis, but not cytokinesis, continues in K cyclin-expressing cells, leading to multinucleation and polyploidy. Such polyploid cells exhibit pronounced centrosome amplification and consequent aneuploidy. Our data suggest that K cyclin expression leads to cytokinesis defects and polyploidy, which activates p53. However, in the absence of p53, such cells survive and expand as an aneuploid population. Corroborating these findings, in vivo Eμ K cyclin expression cooperates with p53 loss in the induction of lymphomas.

Introduction

Infection of human B lymphocytes and endothelial cells with Kaposi's sarcoma-associated herpesvirus (KSHV, a.k.a. HHV-8) predisposes carriers to the development of certain B cell malignancies (primary effusion lymphoma [PEL] and Multicentric Castleman's disease [MCD]) and the skin tumor Kaposi's sarcoma (KS) (Chang et al., 1994). The majority of tumor cells in such neoplasms are latently infected (Boshoff et al., 1995; Zhong et al., 1996), suggesting that latent genes are important for viral pathogenesis. One latently expressed candidate KSHV oncogene encodes K cyclin, which is structurally related to cellular G1 D-type cyclins.

D-type cyclins form active holoenzymes with Cdk4 or Cdk6, and their major role appears to be to initiate inhibitory phosphorylation of the Retinoblastoma (Rb) protein. Subsequent Rb phosphorylation via cyclin E/Cdk2 complexes inactivates Rb and thereby liberates the E2F transcription factors, driving entry into S phase (Lundberg and Weinberg, 1998). However, cyclin E/Cdk2 complexes also have Rb-independent functions, since cyclin E is required for the G1/S transition in Rb-deficient cells (Ohtsubo et al., 1995). Indeed, Cdk2, in complex with either cyclin E or cyclin A, can phosphorylate proteins of the replication machinery like Cdc6, directly activating DNA replication (Jiang et al., 1999).

In vitro studies have shown that KSHV K cyclin can interact with all Cdks, although it favors Cdk6 (Godden-Kent et al., 1997; Jung et al., 1994; Li et al., 1997). Such K cyclin/Cdk complexes are refractory to inhibition by CDK inhibitors (Jeffrey et al., 2000; Swanton et al., 1997). Another unique feature of K cyclin/Cdk6 complexes is that they potently phosphorylate an extended array of substrates that are not normally targets of cellular cyclin D/Cdk6. These include the cyclin E/Cdk2 targets p27^{Kip1}, Id-2, and Cdc25A (Ellis et al., 1999; Mann et al., 1999) and the cyclin A/Cdk2 targets of the replication machinery Cdc6 and Orc1 (Laman et al., 2001). K cyclin phosphorylation of p27^{Kip1} triggers its degradation, further facilitating the activation of endogenous cyclin/Cdk complexes. Thus, the activity of the K cyclin/Cdk6 complex in part mimics the combined activities of G1 and S phase cyclin/Cdk complexes. This is consistent with the ability of K cyclin, unlike cyclin D, to initiate DNA replication in an in vitro replication system (Laman et al., 2001) and to enforce S phase entry in quiescent cells or in cells arrested by CDK inhibitors (Swanton et al., 1997). Such properties of K cyclin support the notion that it can function as an oncogenic protein, although no such role for K cyclin has yet been reported.

In addition to driving cell cycle progression, K cyclin/Cdk6 complexes can, like many other oncogenic proteins, trigger apoptosis (Ojala et al., 1999), although the molecular mechanisms underlying K cyclin-induced apoptosis are largely unknown. Endogenous cell growth-deregulating oncoproteins, such as c-Myc or E2F-1, induce apoptosis via discrete pathways that can sensitize the cell to a wide variety of proapoptotic insults, including ligation of TNF/TRAIL/FAS family death recep-

SIGNIFICANCE

Infection of human B lymphocytes or endothelial cells by Kaposi's sarcoma-associated herpesvirus (KSHV) predisposes carriers to the development of lymphoproliferative disorders and the skin cancer Kaposi's sarcoma. Most such malignant cells are latently infected with KSHV, and K cyclin is one of the few latently expressed genes. K cyclin/Cdk complexes exhibit several unique features that promote proliferation, including resistance to Cdk inhibitors. Our study shows that the tumorigenicity of K cyclin is greatly enhanced in the absence of the p53 tumor suppressor pathway. Furthermore, our finding that the mitogenic effects of K cyclin are antagonized by p53 provides an explanation for the presence of a set of p53-inhibiting proteins in the KSHV genome and suggests that pharmacological disruption of this inhibition may be a potential means of anti-KSHV therapy.

tors and survival factor deprivation (Evan et al., 1992; Hueber et al., 1997; Klefstrom et al., 1997; Phillips et al., 1999). Oncogenic c-Myc is thought to mediate its proapoptotic effect by promoting the release of holo-cytochrome c (cyt c) from the mitochondria into the cytosol (Juin et al., 1999). Interestingly, K cyclin/cdk6 complexes can phosphorylate and inactivate cellular Bcl-2 (Ojala et al., 2000), a key regulator of cytochrome c release from mitochondria, suggesting that K cyclin expression, at least under certain circumstances, may directly interfere with mitochondrial integrity.

Another well-characterized proapoptotic pathway activated by oncoproteins like E2F1, E1A, c-Myc, and Ras is the ARF/p53 pathway (Bates et al., 1998; de Stanchina et al., 1998; Palmero et al., 1998; Zindy et al., 1998). Activation of such oncoproteins can induce upregulation of $p19^{ARF}$ (or human $p14^{ARF}$) protein, which then associates directly with Mdm2 protein and neutralizes its ability to promote the ubiquitination and degradation of p53 (Kamijo et al., 1998; Pomerantz et al., 1998; Zhang et al., 1998). This results in p53 stabilization and consequent cell cycle arrest or apoptosis.

In this study we have explored the consequences of K cyclin expression in human and mouse primary cells. We show that expression of K cyclin in primary cells blocks cytokinesis; yet, it simultaneously drives DNA replication. Our data suggest that the resulting polyploidy, rather than the E2F1/$p19^{ARF}$ pathway, activates p53, thereby triggering growth arrest and apoptosis. Loss of p53 dramatically exacerbates K cyclin-induced lymphomagenesis in vivo, indicating that growth arrest and/or apoptosis induced by K cyclin must be overcome in order for its oncogenic potential to be revealed.

Results

Expression of K cyclin in MEFs sensitizes cells to apoptosis induced by DNA damage, death receptor ligation, and survival factor deprivation

To explore the molecular mechanism of K cyclin-induced apoptosis, we used the pBMNIresEGFP (K cyclin pBMN) retrovirus vector to express K cyclin in early passage mouse embryo fibroblasts (MEFs). This vector dicistronically directs the concomitant expression of K cyclin and green fluorescent protein (GFP). Following transduction, around 80% of the cells were GFP positive, and apoptotic cells in this population were identified by Annexin V-PE and Via-Probe staining using flow cytometric analysis (Figure 1, upper panel). We observed no significant increase in apoptosis in K cyclin-expressing cells grown in 10% FBS (around 8%, compared with 3% upon mock infection) (Figure 1, lower panel). Next, we examined whether expression of K cyclin sensitizes cells to other triggers of apoptosis by subjecting K cyclin-expressing cells to various proapoptotic stimuli for 48 hr. Treatment of control MEFs with low (0.2%) serum, with the DNA damaging agent etoposide, or with TNF or TRAIL induced no significant cell death (around 5%–12% apoptosis) during the course of the experiment: in contrast, all of these insults induced pronounced apoptosis in MEFs expressing K cyclin (Figure 1, lower panel). The sensitization to apoptosis by K cyclin was especially evident in cells grown in 0.2% FBS, where nearly 40% of the K cyclin-expressing cells underwent apoptosis. These data demonstrate that K cyclin expression sensitizes MEFs to the induction of apoptosis by DNA damage, death receptor ligation, and survival factor deprivation.

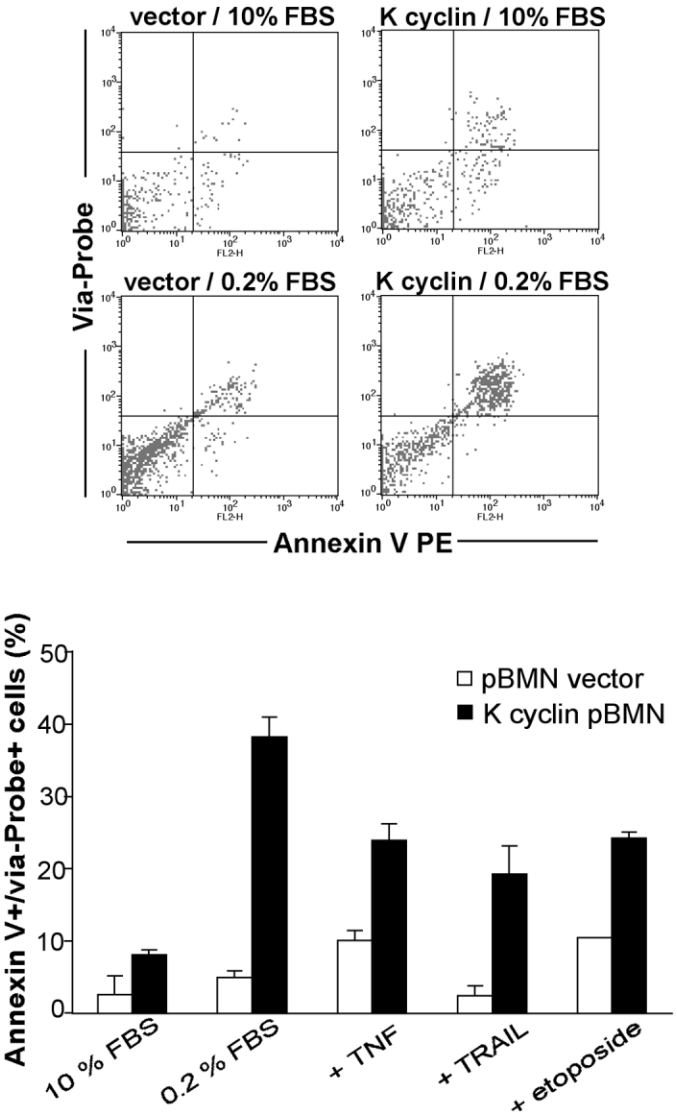

Figure 1. Expression of K cyclin sensitizes MEFs to death triggered by various stress signals

Wt MEFs were infected for 2 subsequent days with KpBMN or empty vector and were next cultured for 48 hr in medium containing 10% FBS, 0.2% FBS, or 10% FBS supplemented with etoposide (5.0 μM), TNF (50 ng/ml), or TRAIL (200 ng/ml). Floating and adhered cells were collected and stained with Annexin V-PE and Via-Probe, followed by flow cytometric analysis, an example of which is shown in the upper panel. The mean percentages of dead cells ± SEM of three independent experiments are shown

K cyclin-induced apoptosis requires p53, but not E2F1 or $p19^{ARF}$

A common mechanism by which oncoproteins trigger apoptosis is via the $p19^{ARF}$/p53 pathway. In human cells, E2F1 directly activates expression of $p14^{ARF}$ by activating transcription from the $p14^{ARF}$ promoter (Bates et al., 1998). Since expression of K cyclin leads to strong phosphorylation of Rb (Child and Mann, 2001) and subsequent release of E2Fs, we asked whether the

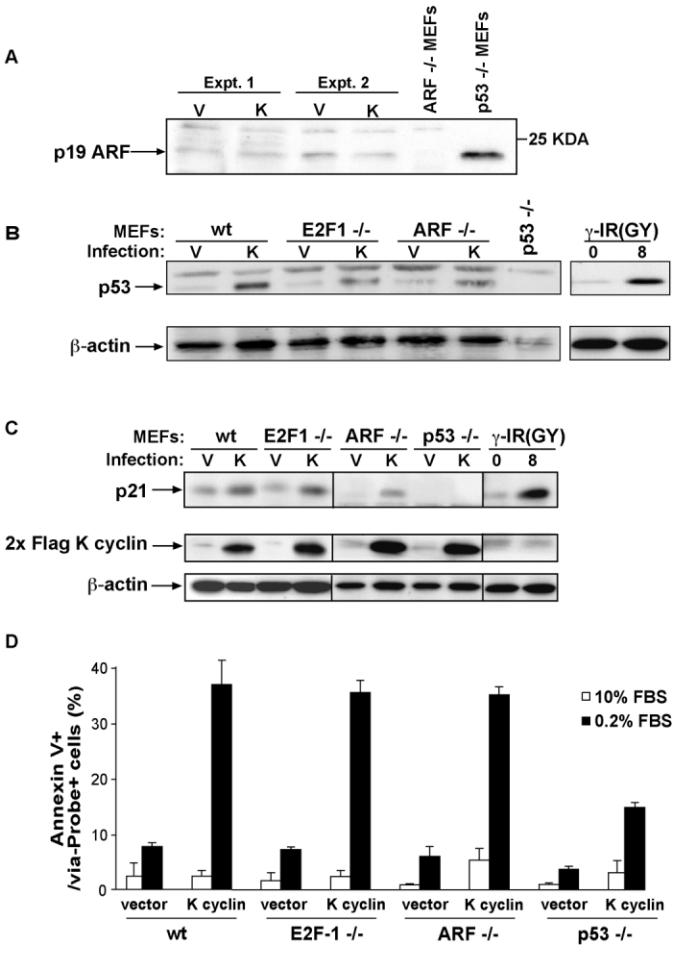

Figure 2. P19^{ARF} and E2F1 expression are dispensable, but p53 is required for apoptosis induced by K cyclin

A: K cyclin does not induce p19^{ARF} expression in MEFs. Wt MEFs were infected with K cyclin-encoding (K) or empty virus (V). Infected cells were selected by puromycin and were grown for 72 hr in medium containing 10% FBS. *p53−/−* MEFs are shown as a positive control, since they contain high levels of endogenous p19^{ARF} due to the lack of a p53-mediated negative feedback loop (Stott et al., 1998). Lysates were prepared and analyzed by immunoblotting with anti-p19^{ARF} antibody. **B:** K cyclin expression is associated with elevated p53 levels. MEFs of the indicated genotype were infected with empty (V) or K cyclin-encoding pBabepuro (K) vector. Infected cells were selected by puromycin and were grown for 72 hr in medium containing 10% FBS until cell lysates were prepared. As a control, a subconfluent culture of wt MEFs was exposed to 8 GY of γ-irradiation and was grown for an additional 24 hr. Proteins were immunoblotted with CM-5 p53 or β-actin antibody. **C:** Protein lysates from MEFs infected as in **B** were analyzed by immunoblotting with anti-Flag antibody to detect tagged K cyclin or with CM-5 p53, p21^{Cip1}, or β-actin antibody. **D:** Wt, *E2F1−/−*, *ARF−/−*, and *p53−/−* MEFs were infected for 2 subsequent days with KpBMN or empty vector, followed by growth for 48 hr in 10% FBS- or 0.2% FBS-containing medium. Cells were stained with Annexin V-PE and Via-Probe and were analyzed by flow cytometry to determine the percentage of apoptotic cells in the GFP-positive cell population.

p19^{ARF} protein level is upregulated in MEFs upon K cyclin expression. K cyclin protein was retrovirally expressed in MEFs growing in 10% FBS, and, 72 hr later, the cells were assayed for p19^{ARF} protein expression by immunoblotting. However, we observed no upregulation of p19^{ARF} protein upon K cyclin expression (Figure 2A).

To examine a potential role for p53 in K cyclin-induced apoptosis, we first analyzed whether p53 protein levels are increased upon K cyclin expression. Retroviral expression of K cyclin in MEFs growing in 10% FBS resulted in an upregulation of p53 protein (Figure 2B). Induction of p53 protein levels correlated with an increase in the levels of the p53 target gene *p21^{Cip1}* (Figure 2C), implying an upregulation of transcriptionally active p53 protein upon K cyclin expression. Strikingly, K cyclin expression in *E2F1−/−* or *ARF−/−* MEFs also resulted in an increase in active p53 protein levels (Figures 2B and 2C). Thus, neither E2F1 nor p19^{ARF} is required for the activation of p53 by K cyclin.

Next, we determined the requirement of p53 in K cyclin-induced apoptosis. K cyclin was transduced into wild-type (wt), *E2F1−/−*, *ARF−/−*, and *p53−/−* MEFs, followed by growth of cells for 48 hr in 0.2% FBS. Levels of apoptosis induced by K cyclin were similar in wt, *E2F1−/−*, and *ARF−/−* MEFs. In contrast, K cyclin induced substantially less apoptosis in *p53−/−* MEFs as compared to wt MEFs (15% in *p53−/−* cells compared to about 38% in other MEFs, Figure 2D). These data show that K cyclin-induced apoptosis does not require p19^{ARF} or E2F1, although a significant component of apoptosis is p53 dependent.

K cyclin expression triggers a p53-dependent, but p21^{Cip1}-independent, growth arrest

During the course of these studies, we noticed that K cyclin-expressing cells exhibited a large and flattened phenotype and that cultures could not be propogated. Oncogenes such as Ras can trigger growth arrest in primary cells (Serrano et al., 1997), and this prompted us to investigate whether K cyclin could also induce growth arrest in MEFs.

We first determined the cell proliferation capacity of mock and K cyclin-transduced MEF populations. Mock-infected wt, *E2F1−/−*, and *ARF−/−* cells proliferated until they reached confluence (Figure 3A, closed symbols), whereas cells transduced with K cyclin (Figure 3A, open symbols) showed no net propagation. No such inhibition of cell proliferation was observed upon ectopic expression of cellular cyclin D3 in wt MEFs, although protein expression was readily detectable by immunoblotting (data not shown). Importantly, K cyclin-expressing *p53−/−* MEFs expanded until confluent, although the proliferation rate was somewhat reduced compared with that in mock-infected cells (Figures 3A and 3B). K cyclin-expressing *p53−/−* MEFs could be kept in culture for at least 3 weeks (data not shown), showing that *p53−/−* MEFs can tolerate the presence of K cyclin for an extended period of time.

The lack of a net propagation of K cyclin-expressing cells might result either from an elevated rate of apoptosis relative to proliferation, or from an absence of proliferation due to a block in cell division. To investigate whether K cyclin blocks cell division, we performed time-lapse videomicroscopy to follow cultures of infected MEFs. Representative QuickTime movies of these experiments can be viewed in the Supplementary Material available with this article online (http://www.cancercell.org/cgi/content/full/2/3/229/DC1). The quantitation of cell divisions in these movies show that, while mock-infected wt MEFs proliferate to confluence, K cyclin-expressing wt, *E2F1−/−*, and *ARF−/−* MEFs failed to divide at all (see Figure 3C for wt MEFs expressing K cyclin). However, *p53−/−* MEFs expressing K cyclin divided and proliferated until confluent (Figure 3C). Taken

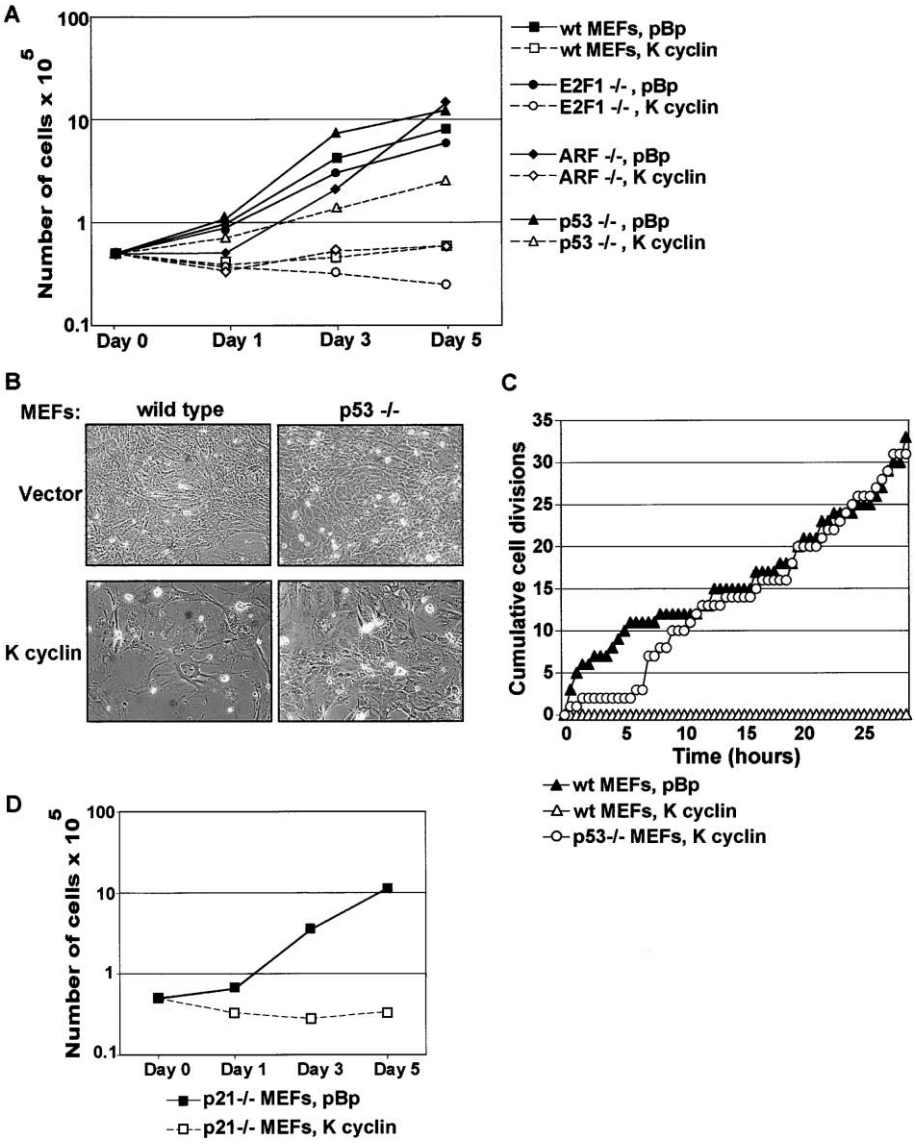

Figure 3. K cyclin-expressing MEFs show a p53-dependent growth arrest

A: Growth curves of MEFs constitutively expressing K cyclin. Wt, *E2F1−/−*, *p53−/−* , or *ARF−/−* MEFs were transduced with empty or K cyclin-encoding pBabepuro retrovirus. Transduced cells were selected by puromycin and were grown in medium containing 10% FBS. Cells were plated at 0.5×10^5 cells per well at day 0, and cell numbers were counted 1, 3, and 5 days later. The experiment was repeated three times with essentially similar results, and the growth curves represent the average of these experiments. **B:** Microscopic analysis of cells at day 5 of the growth curve. Phase-contrast pictures were taken at a magnification of 10×. **C:** Cultures of MEFs transduced and cultured as in **A** were followed by time-lapse videomicroscopy (see the Supplementary Material for QuickTime movies). Pictures were taken every 10 min, and cultures were followed for 4 days. Movies were analyzed for cell divisions, and cumulative cell divisions of wt or *p53−/−* MEFs expressing K cyclin were plotted. **D:** Growth curves of *p21−/−* MEFs infected with empty of K cyclin-encoding pBabepuro retrovirus and analyzed as in **A**.

together, these data imply that constitutive expression of K cyclin not only induces apoptosis but also blocks cell division via a mechanism that does not require E2F1 or $p19^{ARF}$, but does require p53.

p53-dependent growth arrest is often attributed to the Cdk-inhibitory action of the $p21^{Cip1}$ protein (Stewart and Pietenpol, 2001). Since $p21^{Cip1}$ accumulates in cells expressing K cyclin (Figure 2C), we asked whether K cyclin expression results in the arrest of *p21−/−* MEFs. A lack of $p21^{Cip1}$ did not mitigate the K cyclin-induced growth arrest (Figure 3D and Movie S1).

Increase in multincleation and polyploidy upon K cyclin expression

Time-lapse analysis of K cyclin-expressing cells indicated that cells and their nuclei enlarged over time. We also frequently observed that the cell nuclei divided without concomitant cell division, yielding cells with multiple nuclei (Figure 4A). This phenotype was seen in both wild-type and in *p53−/−* MEFs expressing K cyclin, but it was more dramatic in the latter, which exhibited large multilobular nuclei. This suggested to us that, despite defective cell division in K cyclin-expressing cells, DNA replication was still taking place.

To determine whether MEFs arrested upon K cyclin expression maintained DNA synthesis, cells were transduced with K cyclin and were cultured for 3 days in the presence of serum. Subsequently, they were labeled for 5 hr with BrdU and were analyzed by flow cytometry. A significant percentage of cells expressing K cyclin had entered S phase over the course of BrdU labeling (Figure 4B), with percentages being roughly equivalent to mock-infected cultures. To confirm that the observed multinuclear cells had incorporated BrdU, we examined the cells by immunofluorescence microscopy using an anti-BrdU antibody. BrdU staining was observed in the K cyclin-expressing growth-arrested MEFs with large or multiple nuclei (Figure 4C, arrows), indicating that these cells had synthesized DNA.

MEFs comprise a heterogeneous cell population, and some multinucleation and polyploidy occurs spontaneously. We therefore quantitated polyploidy by DNA staining and flow cyto-

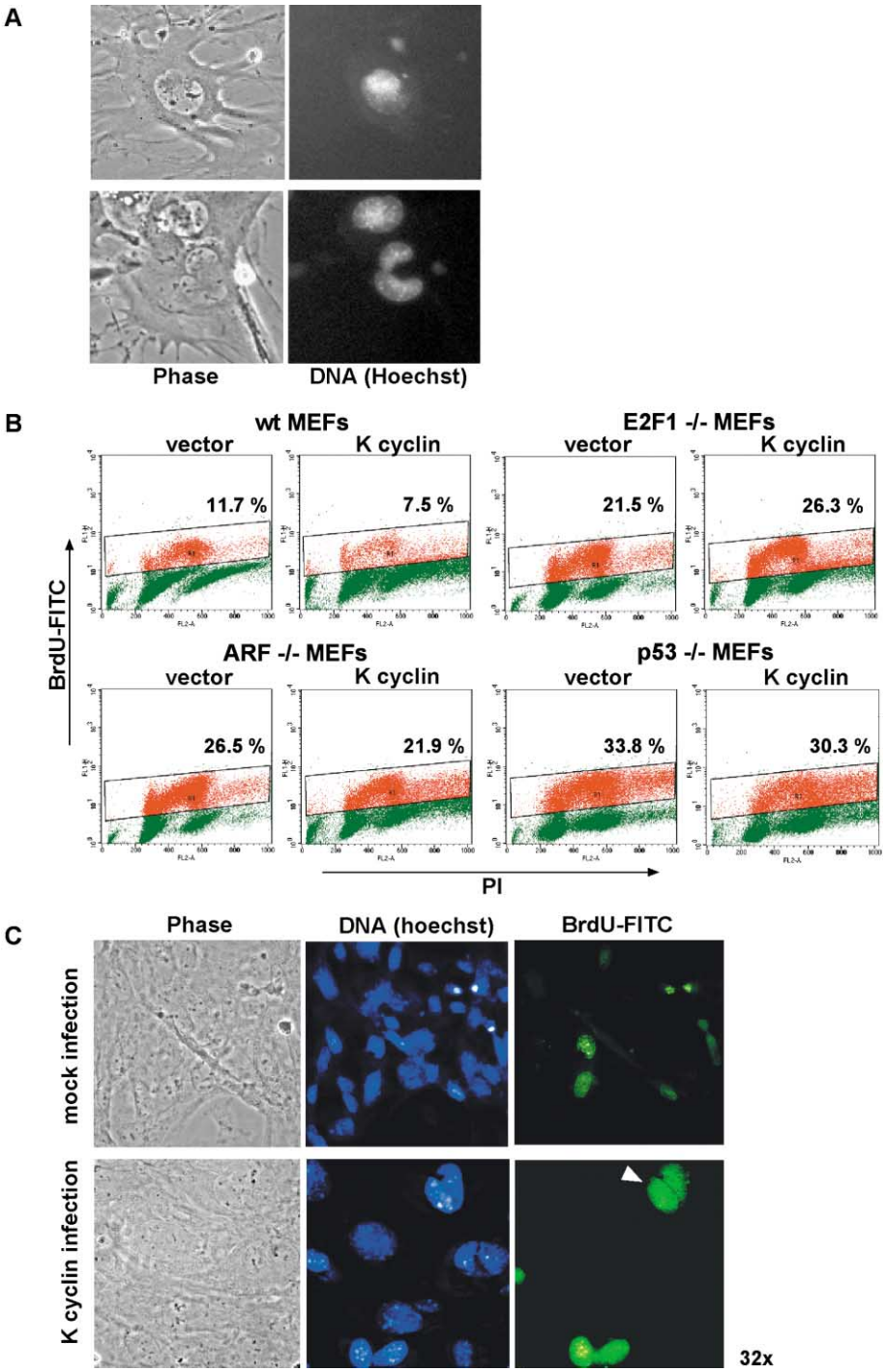

Figure 4. Growth-arrested K cyclin-expressing MEFs synthesize DNA

A: K cyclin-expressing cells become multinucleated. Cultures were infected and grown as in Figure 3A and were microscopically analyzed at day 5 of the growth curve. DNA was counterstained with Hoechst. Pictures were taken at a magnification of 32×. **B:** Wt, *E2F1*−/−, *ARF*−/−, or *p53*−/− MEFs were infected as described in Figure 3A and were grown for 3 days. BrdU (50 μM) was added to the medium, and the cells were grown for an additional 5 hr. Cells were collected and stained with PI and anti-BrdU-FITC conjugate and were analyzed by flow cytometry. The percentages of BrdU-positive cells are indicated. **C:** Cells infected as in Figure 3A were grown on coverslips for 3 days, followed by growth in medium containing BrdU for 5 hr. Cells were fixed in 70% ethanol and were stained with anti-BrdU-FITC (green) and Hoechst (blue) for DNA. Slides were microscopically analyzed, and pictures were taken at a magnification of 32×. A large, multinucleated BrdU-positive cell is indicated with an arrowhead.

metric analysis. Mock- and K cyclin-transduced MEFs were cultured for 3 days in the presence of serum. A significant fraction of wt, *E2F1*−/−, and *ARF*−/− MEFs expressing K cyclin showed increased ploidy, which was reflected by an increase in the fraction of cells with approximately 8N DNA content (from 3%–6% in mock-infected to around 22%–27% in K cyclin-expressing cultures) (Figure 5A). *p53*−/− MEFs showed increased ploidy (~14%) even in control, mock-infected cultures. Importantly, expression of K cyclin also induced accumulation of cells with an 8N DNA content in *p53*−/− MEFs (up to the level of 26%). These data show that a significant proportion of the MEFs expressing K cyclin go through multiple rounds of DNA replication without cell division.

To confirm that the multinucleation and polyploidy induced by K cyclin are not phenomena peculiar to MEFs, we used amphotropic retroviruses to introduce K cyclin into primary human lung fibroblasts. As with MEFs, primary human fibroblasts growth-arrested upon K cyclin expression (Figure 5B, upper panel). This growth arrest was further confirmed by time-lapse videomicroscopy (see the Supplementary Material). Further-

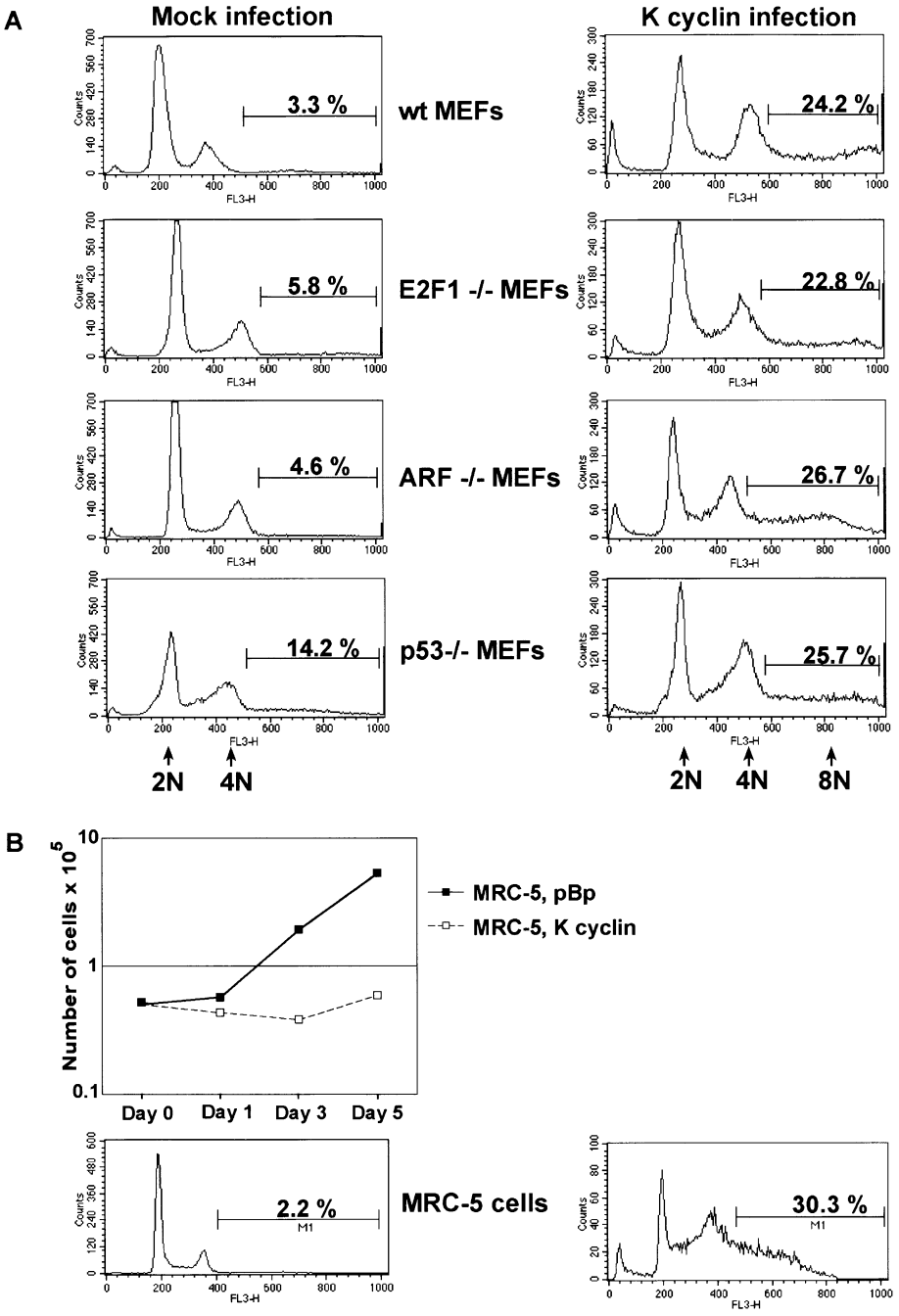

Figure 5. MEFs and MRC-5 cells expressing K cyclin become polyploid

A: MEFs infected and grown as described in Figure 6A were grown for 3 days in 10% FBS-containing medium. Adhered cells were harvested, followed by staining of the DNA with PI and flow cytometric analysis to establish cell cycle profiles. The percentages of cells with a DNA content greater than 4N are indicated. **B:** MRC-5 cells transduced with empty or K cyclin-encoding retrovirus were grown, and growth curves were determined as described in Figure 4A. Cells cultured for 3 days were harvested and analyzed by flow cytometry as in **A**.

more, flow cytometric analysis of K cyclin-expressing human fibroblasts cultured for 3 days in the presence of serum showed the presence of a polyploid population of cells (Figure 5B, lower panel). Taken together, we conclude that K cyclin expression leads to the formation of a polyploid population of cells in both human and mouse primary fibroblasts.

Centrosome amplification in K cyclin-expressing MEFs

It has recently been shown that multinucleated cells often contain more than two centrosomes (Meraldi et al., 2002). Centrosomes constitute the microtubule-organizing centers of the cell and as such assure proper segregation of chromosomes to daughter cells. Centrosome amplifications can result in the formation of multiple spindles and consequent aberrant chromosome separation and genomic instability and, in this way, potentially promote tumorigenesis (Hinchcliffe and Sluder, 2001). Interestingly, the centrosome duplication cycle has been linked to cyclin E/A-driven cdk2 activity (Lacey et al., 1999; Matsumoto et al., 1999; Meraldi et al., 1999). Since many K cyclin-expressing cells are multinucleated and K cyclin/Cdk activity resembles Cdk2 activity, we investigated whether K cyclin-expressing cells exhibit an increased number of centrosomes.

We analyzed the number of centrosomes in K cyclin-expressing cells by immunocytochemical staining of the

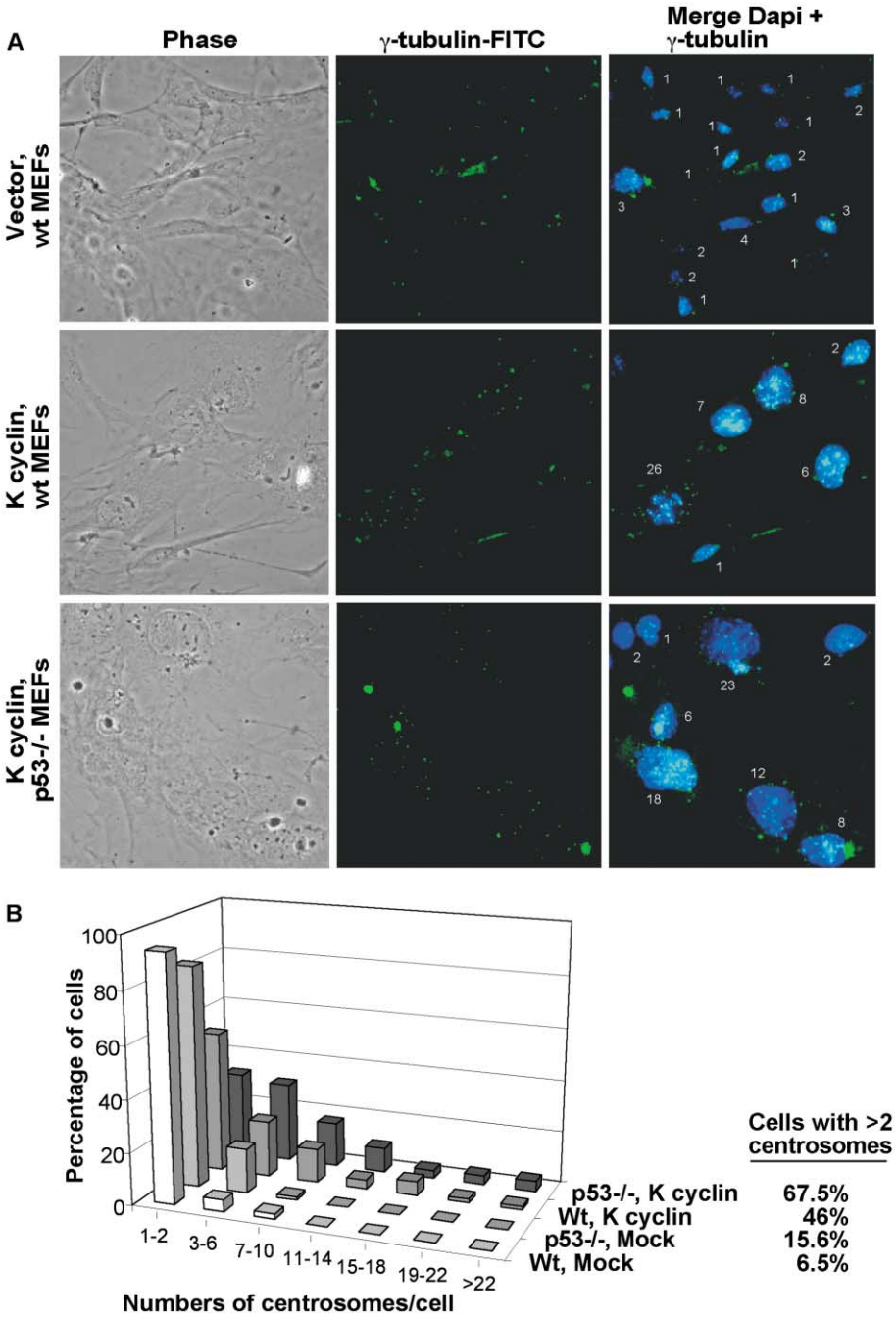

Figure 6. Centrosome amplifications in K cyclin-expressing MEFs

A: Wt or *p53−/−* MEFs were infected with empty or K cyclin-encoding vector, grown for 3 days on coverslips, and stained with anti-γ-tubulin antibody for centrosomes (green) and DAPI (blue) for DNA. The numbersindicate the amounts of centrosomes per cell. **B:** Quantitation of the centrosome analysis described in **A**. The pooled percentages of three experiments of around 70 cells each are shown.

centrosomal proteins γ-tubulin and centrin. Anti-γ-tubulin staining of MEFs expressing K cyclin show a marked increase in the average number of centrosomes per cell above the expected number of 1–2 centrosomes per normal cell (Figures 6A and 6B). While only 6.5% of mock-infected wt or 15.6% of *p53−/−* MEFs had more than two centrosomes, around 46% of wt MEFs expressing K cyclin showed centrosome amplification. Amplification of centrosomes was typically observed in cells with large or multiple nuclei (Figure 6A, middle panel). Loss of p53 exacerbated this phenotype, with around 67.5% of K cyclin-expressing *p53−/−* MEFs showing centrosome amplifications. The actual numbers of centrosomes observed were remarkably high, ranging from 3 to 40 centrosomes per cell. Staining with an anti-centrin antibody showed analogous results, confirming the specific staining of centrosomes (data not shown).

The DNA and centrosome replication cycles are thought to be coregulated. To explore a potential correlation between the number of centrosomes and the DNA content (N) per cell, we quantitated nuclear DNA content using quantitative immunofluorescence microscopy. The normalized DNA content of mock-infected cultures shows values of N ranging from 2 to 4 (Figure 7A), validating the use of our method. In contrast, a significant proportion of K cyclin-expressing cells have a DNA content of around 8N, increasing in a few cells to around 16N,

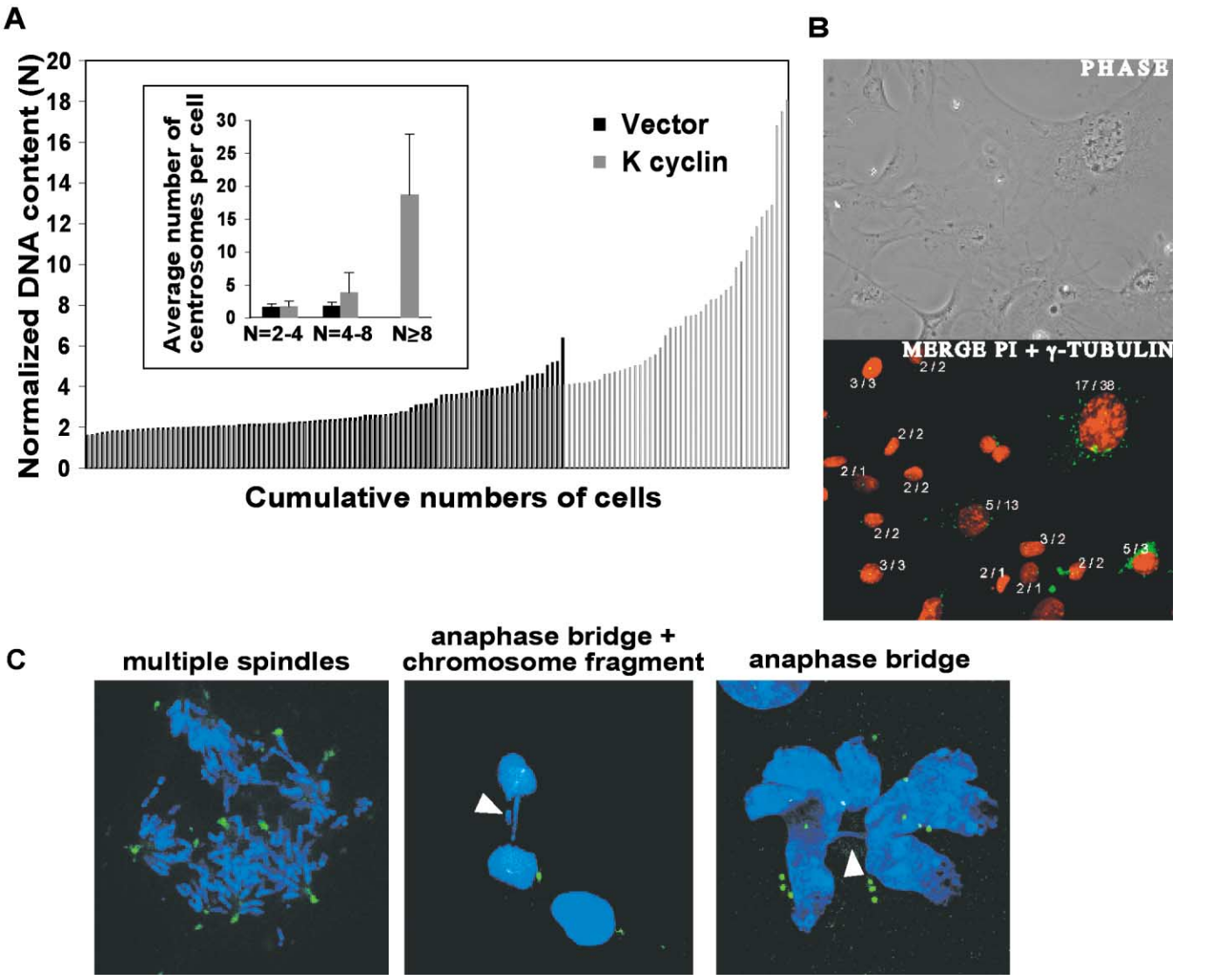

Figure 7. Centrosome amplification correlates with ploidy and is associated with genomic abnormalities

A: Wt MEFs infected and grown as in Figure 7A were stained with anti-γ-tubulin and PI. The DNA content per nucleus was measured by quantitative immunofluorescence microscopy and was normalized to obtain an N = 2 population. Around 100 mock-infected cells or 150 K cyclin-infected cells were analyzed. The inset histogram illustrates that average numbers of centrosomes increase with DNA content. **B:** Example of the correlation analysis. The panel shows a field of wt MEFs infected with K cyclin that were stained with γ-tubulin (green) and PI (red). The numbers before the slash represent DNA contents, and the numbers after the slash represent centrosome counts. **C:** Confocal microsopic analysis of wt (first image) or p53−/− MEFs (second and third image) infected with K cyclin retrovirus and grown and stained as described in **A**. The pictures represent the image layer that best visualized the genomic abnormality, magnification 63× and 2× zoom.

consistent with the flow cytometric analysis (Figure 5). We correlated the DNA content of each individual cell with the number of centrosomes in the same cell (inset in Figure 7A and Figure 7B). Notably, the cells with the highest DNA content contain the highest number of centrosomes. Furthermore, cells with amplified centrosomes are always polyploid (inset in Figure 7A), and these cells often contain a single, but very large, nucleus (Figure 7B).

Primary human fibroblasts also exhibited centrosome amplification upon K cyclin expression, although the numbers of centrosomes per cell were not as high as with MEFs (maximum of six per cell, data not shown). However, the polyploidy in human fibroblasts was also less pronounced (Figure 5B), consistent with the finding that an increase in ploidy correlates with an increase in the number of centrosomes.

The presence of multiple centrosomes in one cell can lead to the formation of multiple spindles and improper chromosome separation. Indeed, confocal studies of our cells revealed the formation of multipolar spindles and, in *p53*−/− cells, anaphase bridges that were sometimes accompanied by chromosomal fragments (Figure 7C). We conclude that K cyclin expression leads to genomic instability, involving increases in ploidy and centrosome amplifications. Furthermore, such genomically unstable cells are viable and are able to expand in the absence

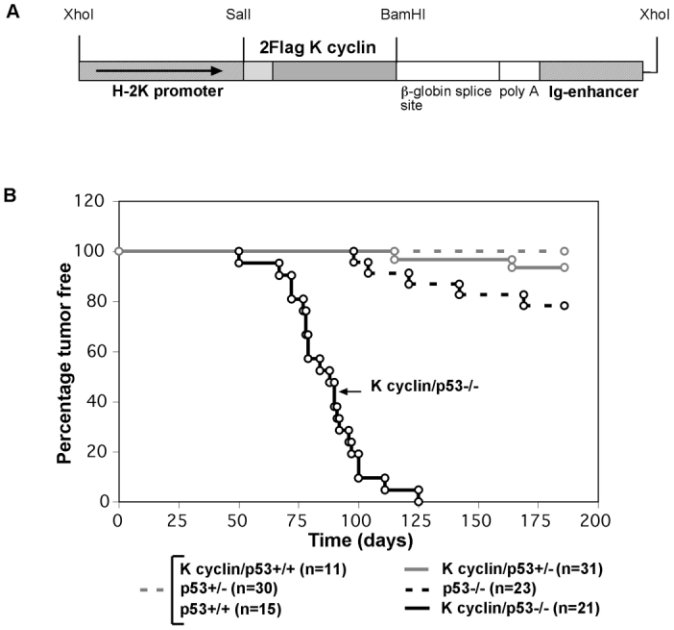

Figure 8. Eμ K cyclin cooperates with p53 loss in tumorigenesis

A: A graphic representation of the transgenic cassette used to generate Eμ K cyclin transgenic founders. **B:** Kaplan Meier survival curves of K cyclin transgenic *p53−/−*, *p53+/−*, or *p53+/+* mice and nontransgenic controls. All *K cyclin/p53−/−* mice developed lymphoblastic lymphomas.

of p53, explaining the exacerbation of the K cyclin-associated phenotype in *p53−/−* MEFs.

Loss of p53 cooperates with K cyclin in murine lymphomagenesis

Our in vitro results show that loss of p53 promotes the survival and outgrowth of K cyclin-expressing cells with unstable genomes. This suggests that K cyclin could be especially tumorigenic in a p53 null background in vivo. To test this hypothesis, we created a transgenic mouse strain expressing K cyclin under the Eμ promoter (Figure 8A). These transgenic mice express K cyclin protein not only in splenic B cells, but also in splenic and thymic T cells. Around 10% of K cyclin transgenic mice develop B or T cell lymphomas by around 7 months of age (E.W.V. et al., unpublished data).

To determine whether loss of p53 exacerbates the oncogenic action of K cyclin in vivo, Eμ K cyclin transgenic mice were bred with *p53−/−* mice, and the progeny of different genotypes were followed for the development of lymphoma. During a 6-month follow-up period, none of the Eμ K cyclin transgenic mice with a *p53+/+* genotype developed tumors. The nontransgenic *p53−/−* mice and the K cyclin-expressing heterozygous *p53+/−* mice developed lymphomas only at very low frequency, with figures of 5/23 (21.7%) and 2/31 (6.5%), respectively. In striking contrast, all Eμ K cyclin transgenic mice with a *p53−/−* genotype rapidly developed T cell (20 mice) or B cell lymphomas (1 mouse) with a mean latency of around 85–90 days (Figure 8B). Thus, the oncogenic potential of K cyclin is revealed in vivo by loss of p53.

Discussion

The unique features of K cyclin/Cdk complexes, including their resistance to Cdk inhibitors and promiscuous phosphorylation of target proteins, are believed to contribute to pathogenesis of KSHV by enhancing the proliferative potential of the host B lymphocytes and endothelial cells latently infected with the virus (Ellis et al., 1999; Mann et al., 1999; Swanton et al., 1997). Despite this, there has been no direct demonstration of an oncogenic function for K cyclin. Our results suggest that the innate oncogenic activity of K cyclin may be suppressed by its induction of p53-dependent apoptosis and growth arrest. Consistent with this, we show for the first time that K cyclin can act as an oncogene in vivo, but only in the absence of the p53 tumor suppressor.

We confirm the previous results of Ojala and colleagues (Ojala et al., 1999) that demonstrated that constitutive expression of K cyclin engages the apoptotic machinery, consistent with the paradigm of activation of dual opposing pathways by oncoproteins. However, while cotransfection of K cyclin with Cdk6 in human cell lines triggered apoptosis directly (Ojala et al., 1999), in our studies, K cyclin expression in mouse embryo fibroblasts elicited little apoptosis alone but acted to sensitize cells to various triggers of apoptosis (Figure 1). Therefore, induction of apoptosis upon K cyclin expression depends on cell

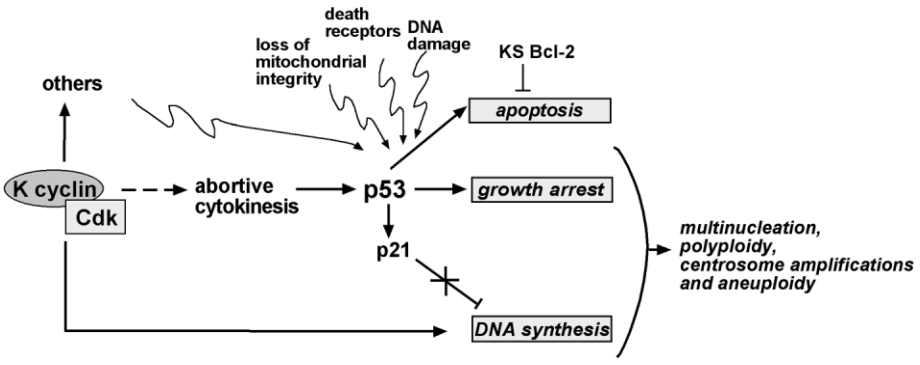

Figure 9. Model showing how expression of K cyclin in MEFs triggers multiple responses

We speculate that cells expressing K cyclin undergo abortive cytokinesis (the mechanism of which is unknown) and adapt from the cytokinesis defect and become tetraploid. This may trigger the activation of p53 and concurrent ($p21^{Cip1}$-independent) growth arrest and sensitization to apoptosis. Because K cyclin is insensitive to the action of Cdk inhibitors such as $p21^{Cip1}$, growth-arrested cells lack functional G1 and G2 checkpoints. This leads to the formation of a polyploid/aneuploid population of cells with amplified centrosomes, which survives and expands in the absence of p53 to become tumorigenic. Additional apoptotic triggers like the phosphorylation and inactivation of endogenous Bcl-2 are likely to contribute to the final fate of K cyclin-expressing cells.

type, and presumably the spectrum of endogenous Cdks and the presence of apoptotic stimuli in the cellular environment.

Expression of K cyclin resulted in the upregulation of transcriptionally active p53 protein and concomitant growth arrest and apoptosis. K cyclin/Cdk complexes stimulate the hyperphosphorylation of Rb and thus catalyze the release of E2Fs, including E2F1, a transcriptional activator of the human $p14^{ARF}$ promoter (Bates et al., 1998). We therefore hypothesized that K cyclin induces p53 stabilization via E2F1-dependent upregulation of $p19^{ARF}$ protein. However, neither the accumulation of p53 protein nor apoptosis or growth arrest upon K cyclin expression requires the presence of either E2F1 or $p19^{ARF}$, implying that K cyclin activates p53 through a different mechanism.

Time-lapse videomicroscopic analysis of K cyclin-expressing cells shows that, although such cells do not divide, many cells still undergo nuclear divisions or contain an enlarged nucleus. In addition, many K cyclin-expressing cells show ongoing DNA replication together with ploidy increase, implying that cells reenter S phase without undergoing cytokinesis. This may relate to the so-called "adaptation" of cells after spindle disruption, in which cells reenter G1 even though cytokinesis is disrupted (Lanni and Jacks, 1998). Interestingly, in such cases, tetraploidy triggers the activation of p53, presumably acting as a safeguard mechanism to eliminate the survival of a polyploid/aneuploid population of cells (Andreassen et al., 2001). Thus, K cyclin-associated tetraploidy may similarly trigger the activation of p53. When cytokinesis is aborted by spindle disruption, p53 arrests the two daughter nuclei in G1 via the induction of the $p21^{Cip}$ protein and inhibition of cyclin/Cdk activity (Andreassen et al., 2001). However, K cyclin/Cdk complexes are refractory to Cdk inhibitors, including $p21^{Cip1}$ (Swanton et al., 1997), and, as a consequence, the p53-induced checkpoint is ignored, such that K cyclin-expressing cells undergo multiple rounds of DNA replication and become polyploid. This situation would be analogous to the endoreduplication upon spindle disruption in *p53*−/− or *p21*−/− cells (Di Leonardo et al., 1997; Khan and Wahl, 1998; Lanni and Jacks, 1998; Stewart et al., 1999) or upon a Ras-induced growth arrest in *p21*−/−/*p27*−/− MEFs (Groth et al., 2000). Taken together, our results favor a model in which p53 is activated upon K cyclin-induced tetraploidy, and not through the E2F1/ARF pathway.

It remains unclear what triggers the cytokinesis defect upon K cyclin expression. Unlike in yeast, where the mechanism of cytokinesis mediated by the "mitotic exit network (MEN)" proteins has been extensively studied, the mode of regulation of cytokinesis in mammalian cells is largely unknown. It is clear, however, that proper orchestration of mitotic cyclin/Cdk activity is essential for cells to undergo cytokinesis. In particular, the mitotic cyclins A and B need to be targeted for degradation via ubiquitination by the anaphase-promoting complex (APC) (Morgan, 1999). We presume that premature or constitutive K cyclin-driven Cdk2-like activity deregulates the timing of the mitotic machinery, thus resulting in defective cytokinesis. Supporting this, recent evidence points at a correlation between the formation of multinucleated cells and deregulated expression of mitotic regulators that impinge either directly on spindle formation or on mitotic cyclin stability (Meraldi et al., 2002; Zhang and Lees, 2001). In addition, the finding that K cyclin-expressing *p53*−/− MEFs continue to divide implies a role for p53 in the regulation of cytokinesis. The possible mechanism is unclear, although it must involve p53-regulated genes other than $p21^{Cip1}$ since *p21*−/− MEFs arrest upon K cyclin expression.

K cyclin-expressing *p53*−/− and wt MEFs show massive centrosome amplification to an extent that has hitherto not been observed. In addition, many K cyclin-expressing cells exhibited multiple spindles and anaphase bridges, indicative of genomic instability. Recently, defects in cell division and concomitant multinucleation were shown to give rise to centrosome amplifications (Meraldi et al., 2002). We also find that many polyploid K cyclin-expressing cells contain amplified numbers of centrosomes. In our case, cells with the highest DNA content often contained one large nucleus (Figure 7B), adding to the model of Meraldi and colleagues in which ploidy, rather than multinucleation, correlates with centrosome number. It therefore seems likely that K cyclin expression promotes chromosome instability via the formation of polyploid cells, although K cyclin may also directly drive centrosome amplifications independent of DNA synthesis.

We suggest that K cyclin expression promotes DNA replication and polyploidy in cells, which then triggers p53-dependent apoptosis and growth arrest (see the model in Figure 9). Thus, in the absence of p53, a polyploid population of cells is able to survive and expand. We therefore hypothesized that K cyclin would promote tumorigenesis only when p53 is absent. This is supported by our transgenic mouse model in which K cyclin expression is regulated by the Eμ promoter. In wild-type mice, a low level of lympoma induction with a long latent period is seen. In contrast, loss of p53 results in a substantial decrease in latency and increases the incidence of K cyclin-induced lymphomas. Loss of p53 leads to inhibition of apoptosis, inhibition of growth arrest, and promotion of aneuploidy, all of which could contribute to K cyclin-induced tumorigenesis. It has recently been suggested that it is the inhibition of apoptosis, rather than the acquisition of aneuploidy, that constitutes the critical tumorigenic effect of p53 loss (Gurova et al., 2002; Schmitt et al., 2002). Whether the same is also true for the exacerbation of K cyclin-induced oncogenicity that we see upon p53 ablation remains to be seen.

In the context of KSHV physiology, it is interesting to note that two of the five latently expressed HHV-8 proteins (LANA and ORF K10) bind p53 and can inhibit its ability to induce transcriptional activation (Friborg et al., 1999; Rivas et al., 2001). Furthermore, LANA has been shown to colocalize with p53 in KS cells (Katano et al., 2001). Thus, our finding that the mitogenic effects of K cyclin are blocked by p53 may offer an explanation for the presence of this set of p53-inhibiting proteins in the KSHV genome. Taken together, our data provide the first evidence for an in vivo oncogenic function of the KSHV cyclin and suggest that the inhibition of the p53 tumor suppressor pathway is an important attribute of K cyclin-induced tumorigenesis.

Experimental procedures

Cell culture and treatment

E2F1−/− (Field et al., 1996), *p53*−/− (Jacks et al., 1994), and *p21*−/− mice (Brugarolas et al., 1995) were obtained from The Jackson Laboratory. $P19^{ARF}$−/− mice were obtained from F. McCormick and were originally from C. Sherr (Kamijo et al., 1997). MEFs from nullizygous and wild-type (C57BL/6 or C57BL/6 × 129) controls were derived from 12- to 14-day-old embryos and were genotyped using PCR protocols supplied by the labs that generated the mice. MEFs were maintained on a 3T9 protocol (Todaro and Green,

1963). Phoenix-Eco and -Ampho retrovirus packaging cells (gift from G. Nolan), MEFs, and MRC-5 primary human lung fibroblasts were maintained in Dulbecco's modified Eagle's medium (DMEM, GIBOCO-BRL), supplemented with 10% fetal bovine serum (FBS), 2 mM glutamine, 100 μg/ml streptomycin, and 100 U/ml penicillin. Cells were cultured at 37°C in 5% CO_2. When indicated, cells were exposed to 8 Gy of γ-irradiation using a Cs irradiator (Mark 1, Model 68 SN.1019, J.L. Shepherd & Associates).

Plasmids

The retroviral vector pBabepuro and double Flag-tagged human cyclin D3 and K cyclin in pBabepuro were gifts from D. Mann. Double Flag-tagged K cyclin was subcloned from KpcDNA3 (Mann et al., 1999) and was ligated in the bicistronic retroviral pBMNIresEGFP vector (gift from F. Rossi), creating KpBMN.

Generation of Eμ K cyclin transgenic mice

Double Flag-tagged *K cyclin* cDNA was amplified by PCR from KpcDNA3 plasmid using primers containing 5′ XhoI and 3′ BamHI sites. Restricted PCR product was ligated into SalI and BamHI cut pHSE3′ plasmid (a generous gift from R. Zinkernagel), creating K cyclin pHSE3, which drives transgene expression from the H-2K promoter/Ig-enhancer cassette (also called Eμ). Expression of K cyclin was confirmed in mouse A20 B cells transiently transfected with K cyclin pHSE3′ plasmid. XhoI-linearized K cyclin PHSE3′ was agarose gel purified using Jetsorb (Genomed), followed by purification using the Wizard DNA clean-up system (Promega). DNA was resuspended at a concentration of 5 ng/μl in sterile injection buffer (10 mM Tris, 0.1 mM EDTA [pH 7.4]), microinjected into the male pronucleus of around 200 fertilized oocytes, and implanted in foster mothers. Potential (CBA × C57BL/6) F1 founder animals were screened for the presence of the *K cyclin* cDNA by Southern blot analysis, and positive animals were outbred to F1 animals to establish founder lines. Two founder lines (called Eμ K cyclin 1996E-H [6] and Eμ K cyclin 2269A.1 [20]) expressing high levels in either the splenic B cells or in the thymic T cells were identified. The results shown here are from founder 1996E-H (6).

Retroviral infection, growth curves, flow cytometric analysis, and apoptosis

Retroviral supernatants were produced by transfection of Phoenix-Eco or Phoenix-Ampho retrovirus-producing cells with 4 μg retroviral vector using Lipofectamine Plus reagent (GIBCO-BRL). Supernatants were harvested 40–48 hr after transfection and filtered, and polybrene (Sigma) was added to a final concentration of 10 μg/ml. Passage 2–4 MEFs were plated at 1×10^5 cells per well in a 6-well plate or 1×10^6 cells per 10-cm dish and were infected the next day with 1 ml/well or 5.5 ml/dish of freshly harvested virus. MRC-5 cells were plated at 1×10^6 cells per 10-cm dish and were infected the next day with 5.5 ml freshly harvested virus. For growth curve analysis or for Western blot analysis (see below), MEF cells were infected for 18–24 hr. MRC-5 cells were infected for 9 hr. Infected MEFs were selected by growth for 48 hr in medium containing 5 μg/ml puromycin. Infected MRC-5 cells were trypsinized and seeded at 1:3 dilution in medium containing 5 μg/ml puromycin. The absence of reverse transcriptase activity in culture supernatants of infected MRC-5 cells was confirmed 72 hr after antibiotic selection using the *Quan*-T-RT assay according to the manufacterer's protocol (Amersham). MEFs or MRC-5 cells were plated at a density of 0.5×10^5 cells per well in 6-well plates and were counted at 1, 3, and 5 days after plating to establish growth curves. Alternatively, DNA was stained with Hoechst 33342 dye (Sigma), followed by microscopic analysis.

To assess the effect of K cyclin expression on DNA content, cells infected as above were plated at a density of 0.8×10^6 cells per 10-cm dish (MEFs) or 0.5×10^5 cells per well (MRC-5) and were grown for 3 days until harvesting. Cells were washed twice with PBS and were fixed in 70% ethanol. Cells were resuspended in PBS containing 10 μg/ml propidium iodide (PI), 100 U/ml Ribonuclease A (Sigma), and 0.1% glucose (Sigma) and were immediately analyzed by flow cytometry.

For apoptosis assays, MEFs were infected for 8 hr with fresh pBMNIres-EGFP virus supernatant, followed by overnight incubation in normal growth medium. Phoenix cells were replenished with fresh medium to produce an additional 24 hr viral supernatant, with which a second 8-hr infection was performed the next day. Infected cells were subsequently grown for 48 hr in medium containing 10% FBS, 0.2% FBS, mouse TNF-α (50 ng/ml, specific activity 1.2×10^7 U/mg, kindly provided by Boehringer-Ingelheim), His-tagged TRAIL (200 ng/ml, R&D Systems), or etoposide (5 μM, Sigma) to trigger apoptosis. TRAIL ligand was preincubated for 30 hr at room temperature with 3 μg anti-6x Histidine antibody (R&D systems) to initiate ligand trimerization. Cells and supernatants were collected and stained with Annexin V-PE (Pharmingen) according to the manufacturer's protocol. DNA was counterstained with Via-Probe (20 μl per sample, Pharmingen). The percentage of Annexin V-positive/Via-Probe positive or negative cells in the GFP-expressing population of cells was determined by flow cytometric analysis.

Time-lapse videomicroscopic analysis of cells

MEFs or MRC-5 cells were plated at 1×10^5 cells per well in a 6-well plate. Cells were grown in a humidified system adapted with a CTI-controller (5% CO_2) and a 37-2 digital Tempcontrol (37°C) on an Axiovert S 100 microscope (all systems from Zeiss). About 20–40 cells were followed over the course of 4 days while taking photos (magnification 10×) every 10 min using an Openlab automator module (Improvision). Time-lapse videos were compiled in Openlab and were converted to QuickTime movies (0.1 s per frame).

Immunoblotting of cell lysates

Cells were washed with PBS and were lysed in boiling lysis buffer (2.5% SDS in 0.5 M Tris-HCl [pH 6.8]). Lysates were sonicated and cleared by centrifugation. Protein concentrations were determined using a BioRad DC assay according to the manufacturer's protocol. Proteins (20 μg) were fractionated by SDS-PAGE and were transferred to PVDF membranes (Millipore). Membranes were probed with polyclonal antibodies directed to mouse p53 (CM5, Novocastra), $p19^{ARF}$ (AbCam), or $p21^{Cip1}$ (Pharmingen) or monoclonal antibodies directed to Flag (M2, Sigma) or β-actin (Sigma). Antibody binding was visualized by enhanced chemiluminescence (ECL).

Centrosome immunohistochemistry and DNA quantitation

MEFs grown on coverslips were fixed in ice-cold methanol for 6 min at −20°C. Coverslips were washed with PBS, and cells were permeabilized in 0.1% Tween-20/PBS, followed by staining for 1 hr at room temperature with anti γ-tubulin (1:150, Sigma) or anti-centrin (1:500, generous gift from J.L. Salisbury) primary antibody diluted in 0.5% NP-40/10% goat serum/PBS. After washing and another permeabilization step, primary antibody binding was detected using a donkey anti-mouse Alexa Fluor 488 goat anti-mouse secondary antibody (1:200, Molecular Probes). DNA was counterstained with DAPI (4',6-diamidino-2-phenylindole, 0.5 μM, Sigma), and coverslips were mounted in MOWIOL (Calbiochem), followed by microscopic analysis. Around 70 cells from three experiments were analyzed, and the data were pooled to calculate averages. When indicated, slides were analyzed by confocal microscopy using a Zeiss LSM 510 META microscope.

For quantitation of cellular DNA contents, DNA was counterstained with PI (3 μg/ml, 100 U/ml Ribonuclease A) for 30 min at room temperature. Immunofluoresence microscopy was performed, and the DNA content of individual nuclei was measured using the particle analysis tool of Scion Image 1.62c software by integrating the PI signal density of separate particle. Overlapping nuclei or nuclei touching the edges were ignored. Identical threshold limits were used for all analyses to standardize background signals.

DNA replication analysis

For measurements of DNA replication, cells were infected and grown for 3 days essentially as described for growth curve analysis. A total of 50 μM of 5-bromodeoxyuridine (BrdU, Sigma) was added to the medium, and cells were grown for an additional 5 hr. For flow cytometric analysis, cells were trypsinized, washed twice in 1% BSA/PBS, fixed with cold 70% ethanol, and stored at −20°C. For microscopic analysis, cells grown on coverslips were fixed with 70% ethanol for 30 min at room temperature. BrdU incorporation was determined with an anti-BrdU-FITC conjugate (Becton Dickinson) according to the manufacturer's protocol. BrdU incorporation was measured by flow cytometric analysis or fluorescence microscopy.

Acknowledgments

We thank Drs. D. Mann, F. Rossi, and R. Zinkernagel for providing expression constructs, A. Finch for setting up the time-lapse videomicroscopy system, T. Dansen for help with DNA quantitations, members of the Cancer Center

Laboratory of Cell Analysis core for help with flow cytometry, members of the Imperial Cancer Research Fund (ICRF) transgenic core for generation and maintenance of transgenic mice, F. Rostker for breeding and health checks of the mice, members of the Jones and Evan lab for helpful discussions, and D. Stokoe for editorial comments. This work was supported by the ICRF and generous start-up grants from the UCSF Cancer Research Institute.

Received: July 26, 2002
Revised: August 16, 2002

References

Andreassen, P.R., Lohez, O.D., Lacroix, F.B., and Margolis, R.L. (2001). Tetraploid state induces p53-dependent arrest of nontransformed mammalian cells in G1. Mol. Biol. Cell *12*, 1315–1328.

Bates, S., Phillips, A.C., Clark, P.A., Stott, F., Peters, G., Ludwig, R.L., and Vousden, K.H. (1998). p14ARF links the tumour suppressors RB and p53. Nature *395*, 124–125.

Boshoff, C., Schulz, T.F., Kennedy, M.M., Graham, A.K., Fisher, C., Thomas, A., McGee, J.O., Weiss, R.A., and O'Leary, J.J. (1995). Kaposi's sarcoma-associated herpesvirus infects endothelial and spindle cells. Nat. Med. *1*, 1274–1278.

Brugarolas, J., Chandrasekaran, C., Gordon, J.I., Beach, D., Jacks, T., and Hannon, G.J. (1995). Radiation-induced cell cycle arrest compromised by p21 deficiency. Nature *377*, 552–557.

Chang, Y., Cesarman, E., Pessin, M.S., Lee, F., Culpepper, J., Knowles, D.M., and Moore, P.S. (1994). Identification of herpesvirus-like DNA sequences in AIDS-associated Kaposi's sarcoma. Science *266*, 1865–1869.

Child, E.S., and Mann, D.J. (2001). Novel properties of the cyclin encoded by Human Herpesvirus 8 that facilitate exit from quiescence. Oncogene *20*, 3311–3322.

de Stanchina, E., McCurrach, M.E., Zindy, F., Shieh, S.Y., Ferbeyre, G., Samuelson, A.V., Prives, C., Roussel, M.F., Sherr, C.J., and Lowe, S.W. (1998). E1A signaling to p53 involves the p19(ARF) tumor suppressor. Genes Dev. *12*, 2434–2442.

Di Leonardo, A., Khan, S.H., Linke, S.P., Greco, V., Seidita, G., and Wahl, G.M. (1997). DNA rereplication in the presence of mitotic spindle inhibitors in human and mouse fibroblasts lacking either p53 or pRb function. Cancer Res. *57*, 1013–1019.

Ellis, M., Chew, Y.P., Fallis, L., Freddersdorf, S., Boshoff, C., Weiss, R.A., Lu, X., and Mittnacht, S. (1999). Degradation of p27(Kip) cdk inhibitor triggered by Kaposi's sarcoma virus cyclin-cdk6 complex. EMBO J. *18*, 644–653.

Evan, G.I., Wyllie, A.H., Gilbert, C.S., Littlewood, T.D., Land, H., Brooks, M., Waters, C.M., Penn, L.Z., and Hancock, D.C. (1992). Induction of apoptosis in fibroblasts by c-myc protein. Cell *69*, 119–128.

Field, S.J., Tsai, F.Y., Kuo, F., Zubiaga, A.M., Kaelin, W.G., Jr., Livingston, D.M., Orkin, S.H., and Greenberg, M.E. (1996). E2F–1 functions in mice to promote apoptosis and suppress proliferation. Cell *85*, 549–561.

Friborg, J., Jr., Kong, W., Hottiger, M.O., and Nabel, G.J. (1999). p53 inhibition by the LANA protein of KSHV protects against cell death. Nature *402*, 889–894.

Godden-Kent, D., Talbot, S.J., Boshoff, C., Chang, Y., Moore, P., Weiss, R.A., and Mittnacht, S. (1997). The cyclin encoded by Kaposi's sarcoma-associated herpesvirus stimulates cdk6 to phosphorylate the retinoblastoma protein and histone H1. J. Virol. *71*, 4193–4198.

Groth, A., Weber, J.D., Willumsen, B.M., Sherr, C.J., and Roussel, M.F. (2000). Oncogenic Ras induces p19ARF and growth arrest in mouse embryo fibroblasts lacking p21Cip1 and p27Kip1 without activating cyclin D-dependent kinases. J. Biol. Chem. *275*, 27473–27480.

Gurova, K.V., Kwek, S.S., Koman, I.E., Komarov, A.P., Kandel, E., Nikiforov, M.A., and Gudkov, A.V. (2002). Apoptosis inhibitor as a suppressor of tumor progression: expression of Bcl-2 eliminates selective advantages for p53-deficient cells in the tumor. Cancer Biol. Therapy *1*, 39–44.

Hinchcliffe, E.H., and Sluder, G. (2001). "It takes two to tango": understanding how centrosome duplication is regulated throughout the cell cycle. Genes Dev. *15*, 1167–1181.

Hueber, A.O., Zornig, M., Lyon, D., Suda, T., Nagata, S., and Evan, G.I. (1997). Requirement for the CD95 receptor-ligand pathway in c-Myc-induced apoptosis. Science *278*, 1305–1309.

Jacks, T., Remington, L., Williams, B.O., Schmitt, E.M., Halachmi, S., Bronson, R.T., and Weinberg, R.A. (1994). Tumor spectrum analysis in p53-mutant mice. Curr. Biol. *4*, 1–7.

Jeffrey, P.D., Tong, L., and Pavletich, N.P. (2000). Structural basis of inhibition of CDK-cyclin complexes by INK4 inhibitors. Genes Dev. *14*, 3115–3125.

Jiang, W., Wells, N.J., and Hunter, T. (1999). Multistep regulation of DNA replication by Cdk phosphorylation of HsCdc6. Proc. Natl. Acad. Sci. USA *96*, 6193–6198.

Juin, P., Hueber, A.O., Littlewood, T., and Evan, G. (1999). c-Myc-induced sensitization to apoptosis is mediated through cytochrome c release. Genes Dev. *13*, 1367–1381.

Jung, J.U., Stager, M., and Desrosiers, R.C. (1994). Virus-encoded cyclin. Mol. Cell. Biol. *14*, 7235–7244.

Kamijo, T., Weber, J.D., Zambetti, G., Zindy, F., Roussel, M.F., and Sherr, C.J. (1998). Functional and physical interactions of the ARF tumor suppressor with p53 and Mdm2. Proc. Natl. Acad. Sci. USA *95*, 8292–8297.

Kamijo, T., Zindy, F., Roussel, M.F., Quelle, D.E., Downing, J.R., Ashmun, R.A., Grosveld, G., and Sherr, C.J. (1997). Tumor suppression at the mouse INK4a locus mediated by the alternative reading frame product p19ARF. Cell *91*, 649–659.

Katano, H., Sato, Y., and Sata, T. (2001). Expression of p53 and human herpesvirus-8 (HHV-8)-encoded latency-associated nuclear antigen with inhibition of apoptosis in HHV-8-associated malignancies. Cancer *92*, 3076–3084.

Khan, S.H., and Wahl, G.M. (1998). p53 and pRb prevent rereplication in response to microtubule inhibitors by mediating a reversible G1 arrest. Cancer Res. *58*, 396–401.

Klefstrom, J., Arighi, E., Littlewood, T., Jaattela, M., Saksela, E., Evan, G.I., and Alitalo, K. (1997). Induction of TNF-sensitive cellular phenotype by c-Myc involves p53 and impaired NF-kappaB activation. EMBO J. *16*, 7382–7392.

Lacey, K.R., Jackson, P.K., and Stearns, T. (1999). Cyclin-dependent kinase control of centrosome duplication. Proc. Natl. Acad. Sci. USA *96*, 2817–2822.

Laman, H., Coverley, D., Krude, T., Laskey, R., and Jones, N. (2001). Viral cyclin-cyclin-dependent kinase 6 complexes initiate nuclear DNA replication. Mol. Cell. Biol. *21*, 624–635.

Lanni, J.S., and Jacks, T. (1998). Characterization of the p53-dependent postmitotic checkpoint following spindle disruption. Mol. Cell. Biol. *18*, 1055–1064.

Li, M., Lee, H., Yoon, D.W., Albrecht, J.C., Fleckenstein, B., Neipel, F., and Jung, J.U. (1997). Kaposi's sarcoma-associated herpesvirus encodes a functional cyclin. J. Virol. *71*, 1984–1991.

Lundberg, A.S., and Weinberg, R.A. (1998). Functional inactivation of the retinoblastoma protein requires sequential modification by at least two distinct cyclin-cdk complexes. Mol. Cell. Biol. *18*, 753–761.

Mann, D.J., Child, E.S., Swanton, C., Laman, H., and Jones, N. (1999). Modulation of p27(Kip1) levels by the cyclin encoded by Kaposi's sarcoma-associated herpesvirus. EMBO J. *18*, 654–663.

Matsumoto, Y., Hayashi, K., and Nishida, E. (1999). Cyclin-dependent kinase 2 (Cdk2) is required for centrosome duplication in mammalian cells. Curr. Biol. *9*, 429–432.

Meraldi, P., Honda, R., and Nigg, E.A. (2002). Aurora-A overexpression reveals tetraploidization as a major route to centrosome amplification in p53(−/−) cells. EMBO J. *21*, 483–492.

Meraldi, P., Lukas, J., Fry, A.M., Bartek, J., and Nigg, E.A. (1999). Centrosome duplication in mammalian somatic cells requires E2F and Cdk2-cyclin A. Nat. Cell Biol. *1*, 88–93.

Morgan, D.O. (1999). Regulation of the APC and the exit from mitosis. Nat. Cell Biol. *1*, E47–E53.

Ohtsubo, M., Theodoras, A.M., Schumacher, J., Roberts, J.M., and Pagano, M. (1995). Human cyclin E, a nuclear protein essential for the G1-to-S phase transition. Mol. Cell. Biol. *15*, 2612–2624.

Ojala, P.M., Tiainen, M., Salven, P., Veikkola, T., Castanos-Velez, E., Sarid, R., Biberfeld, P., and Makela, T.P. (1999). Kaposi's sarcoma-associated herpesvirus-encoded v-cyclin triggers apoptosis in cells with high levels of cyclin-dependent kinase 6. Cancer Res. *59*, 4984–4989.

Ojala, P.M., Yamamoto, K., Castanos-Velez, E., Biberfeld, P., Korsmeyer, S.J., and Makela, T.P. (2000). The apoptotic v-cyclin-CDK6 complex phosphorylates and inactivates Bcl-2. Nat. Cell Biol. *2*, 819–825.

Palmero, I., Pantoja, C., and Serrano, M. (1998). p19ARF links the tumour suppressor p53 to Ras. Nature *395*, 125–126.

Phillips, A.C., Ernst, M.K., Bates, S., Rice, N.R., and Vousden, K.H. (1999). E2F-1 potentiates cell death by blocking antiapoptotic signaling pathways. Mol. Cell *4*, 771–781.

Pomerantz, J., Schreiber-Agus, N., Liegeois, N.J., Silverman, A., Alland, L., Chin, L., Potes, J., Chen, K., Orlow, I., Lee, H.W., et al. (1998). The Ink4a tumor suppressor gene product, p19Arf, interacts with MDM2 and neutralizes MDM2's inhibition of p53. Cell *92*, 713–723.

Rivas, C., Thlick, A.E., Parravicini, C., Moore, P.S., and Chang, Y. (2001). Kaposi's sarcoma-associated herpesvirus LANA2 is a B-cell-specific latent viral protein that inhibits p53. J. Virol. *75*, 429–438.

Schmitt, C.A., Fridman, J.S., Yang, M., Baranov, E., Hoffman, R.M., and Lowe, S.W. (2002). Dissecting p53 tumor suppressor functions in vivo. Cancer Cell *1*, 289–298.

Serrano, M., Lin, A.W., McCurrach, M.E., Beach, D., and Lowe, S.W. (1997). Oncogenic ras provokes premature cell senescence associated with accumulation of p53 and p16INK4a. Cell *88*, 593–602.

Stewart, Z.A., Leach, S.D., and Pietenpol, J.A. (1999). p21(Waf1/Cip1) inhibition of cyclin E/Cdk2 activity prevents endoreduplication after mitotic spindle disruption. Mol. Cell. Biol. *19*, 205–215.

Stewart, Z.A., and Pietenpol, J.A. (2001). p53 signaling and cell cycle checkpoints. Chem. Res. Toxicol. *14*, 243–263.

Stott, F.J., Bates, S., James, M.C., McConnell, B.B., Starborg, M., Brookes, S., Palmero, I., Ryan, K., Hara, E., Vousden, K.H., and Peters, G. (1998). The alternative product from the human CDKN2A locus, p14(ARF), participates in a regulatory feedback loop with p53 and MDM2. EMBO J. *17*, 5001–5014.

Swanton, C., Mann, D.J., Fleckenstein, B., Neipel, F., Peters, G., and Jones, N. (1997). Herpes viral cyclin/Cdk6 complexes evade inhibition by CDK inhibitor proteins. Nature *390*, 184–187.

Todaro, G.J., and Green, H. (1963). Quantitative studies of growth of mouse embryo cells in culture and their development into established lines. J. Cell Biol. *17*, 299–313.

Zhang, Y., and Lees, E. (2001). Identification of an overlapping binding domain on Cdc20 for Mad2 and anaphase-promoting complex: model for spindle checkpoint regulation. Mol. Cell. Biol. *21*, 5190–5199.

Zhang, Y., Xiong, Y., and Yarbrough, W.G. (1998). ARF promotes MDM2 degradation and stabilizes p53: ARF-INK4a locus deletion impairs both the Rb and p53 tumor suppression pathways. Cell *92*, 725–734.

Zhong, W., Wang, H., Herndier, B., and Ganem, D. (1996). Restricted expression of Kaposi sarcoma-associated herpesvirus (human herpesvirus 8) genes in Kaposi sarcoma. Proc. Natl. Acad. Sci. USA *93*, 6641–6646.

Zindy, F., Eischen, C.M., Randle, D.H., Kamijo, T., Cleveland, J.L., Sherr, C.J., and Roussel, M.F. (1998). Myc signaling via the ARF tumor suppressor regulates p53-dependent apoptosis and immortalization. Genes Dev. *12*, 2424–2433.